ELSEVIER

Surface and Coatings Technology 124 (2000) 97–103

SURFACE & COATINGS TECHNOLOGY

www.elsevier.nl/locate/surfcoat

An investigation of unbalanced-magnetron sputtered TiAlN films on SKH51 high-speed steel

S.K. Wu [a,*], H.C. Lin [b], P.L. Liu [a]

[a] *Institute of Materials Science and Engineering, National Taiwan University, Taipei 106, Taiwan*
[b] *Department of Materials Science, Feng Chia University, Taichung 407, Taiwan*

Received 22 March 1999; accepted in revised form 6 November 1999

Abstract

A thin coating of TiAlN was deposited on SKH51 high-speed steel using an unbalanced-magnetron sputtering process. The chemical composition, microstructure and mechanical properties of deposited TiAlN films were investigated. The Ti/Al ratio of TiAlN films can be successfully predicted from the sputtering parameters, involving the applied target currents, the yielding of targets impinged by Ar ions and the target configurations. When Ti atoms are partially replaced by Al atoms during the deposition, TiAlN films are identified as a δ-TiN structure and have the preferred texture of the (200) plane. The more internal stress occurring within the deposited TiAlN films is suggested to result in adhesion of TiAlN films inferior to that of TiN films under the same sputtering condition. TiAlN film with a 50% Ti fraction exhibits an excellent cutting performance due to the slight adhesion of SKS-95 steel fragments during the cutting process. © 2000 Elsevier Science S.A. All rights reserved.

Keywords: Composition; Mechanical property; Microstructure; TiAlN; Unbalanced-magnetron sputtering

1. Introduction

Titanium aluminum nitride (TiAlN) has been developed as a coating material [1,2]. The feasibility of using physical vapor deposited (PVD) TiAlN as a coating material for cutting tools has been examined previously [3,4]. The cutting tool materials coated with TiAlN films exhibit an excellent cutting performance, involving higher wear resistance and cutting speed. TiAlN could be successfully synthesized through reactive PVD methods [5–7], such as sputtering, evaporation or ion-plating. Among these techniques, magnetron sputtering is the most attractive due to its higher deposition rate. However, the substrate–target distance of magnetron sputtering is still too inadequate to effectively improve the composition homogeneity of deposition film by adjusting the magnetron strength.

Window and Savvides [8] developed an unbalanced-magnetron sputtering technique to improve the homogeneity of deposition film by increasing the region of homogeneous plasma and the substrate–target distance. This unbalanced-magnetron sputtering technique has been used successfully to deposit various coating materials on cutting tools. However, few investigations have been carried out on the unbalanced-magnetron sputtered TiAlN films. In a sputtering process, the composition and microstructure of deposited films are highly dependent on the substrate temperature, bias, gas pressure, nitrogen flow and sputtering power [9–12]. However, research is minimal concerning the correlation between the sputtering parameters and the optimum properties of the unbalanced-magnetron sputtered TiAlN films. In the present study, SKH51 high-speed steel (HSS) tool material was chosen as a substrate material for coating TiAlN films, which were deposited using closed-field unbalanced-magnetron sputtering [13]. The effects of substrate bias, target current and configuration of Ti/Al targets on the chemical composition, microstructure and mechanical properties of the TiAlN coating are investigated.

2. Experimental procedure

2.1. Sample preparation

TiAlN films were deposited on SKH51 HSS substrates through a four-target closed-field unbalanced-

* Corresponding author. Tel.: +886-2-2363-0231; fax: +886-2-2363-4562.
E-mail address: skw@ccms.ntu.edu.tw (S.K. Wu)

0257-8972/00/$ - see front matter © 2000 Elsevier Science S.A. All rights reserved.
PII: S0257-8972(99)00636-2

Table 1
Chemical composition of SKH51 substrate (wt%)

C	Si	Mn	P	S	Cr	Mo	W	V	Fe
0.80–0.90	<0.40	<0.40	<0.40	<0.40	0.80–4.50	1.50–5.50	5.50–6.70	1.60–2.20	balance

Table 2
The sputtering parameters used in this study, involving configurations of Ti/Al targets, electrical currents of Ti and Al targets and the voltage of substrate bias. The coating thickness of TiAlN film for each specimen is also listed

Specimen No.	Configuration of targets	Ti current (A)	Al current (A)	Substrate bias (V)	Coating thickness (μm)
1	3Ti–1Al	5	7	60	2.6
2	3Ti–1Al	6	7	60	2.5
3	3Ti–1Al	6	5	60	2.7
4	3Ti–1Al	4	7	60	1.8
5	3Ti–1Al	5	7	120	2.3
6	3Ti–1Al	5	7	40	2.6
7	2Ti–2Al	7	4.5	60	2.1
8	2Ti–2Al	7	4.5	90	2.1
9	3Ti–1Al	7	5	60	2.5

magnetron sputtering technique. The equipment used was a UDP450 type made by Teer Co., UK. The chemical composition of the SKH51 substrate is listed in Table 1. The substrates (size: $30 \times 35 \times 6$ mm^3) were finely polished to the surface roughness $Ra \leq 0.01$ μm, degreased, ultrasonically cleaned in liquid Freon, and then blown dry using Freon vapor. The configurations of four Ti/Al targets, 3Ti–1Al and 2Ti–2Al used in the UDP450 sputtering apparatus, are illustrated in Fig. 1. The sputtering was carried out in a mixed Ar–N_2 atmosphere with a substrate rotation of 1.2 rpm and a target–substrate distance of 13–14 cm. A diffusion pump coupled with a rotary pump was used to achieve an ultimate pressure of 5×10^{-5} Torr before introducing the gas mixtures. The substrates were pre-sputtered under an argon discharge of 3.6×10^{-3} Torr for 40 min prior to film deposition. The Ti and TiN interlayers were pre-deposited on the SKH51 substrate before deposition of the TiAlN film. The optical emission monitor (OEM) system was used to detect and control the flow rate of reactive N_2 gas. The optical emission intensity (OES) was set at 50% in this experiment. The sputtering parameters, involving the configurations of Ti/Al targets, electrical currents of Ti and Al targets and the voltage of substrate bias are presented in Table 2. The coating thicknesses of TiAlN films used in this study are also listed in Table 2.

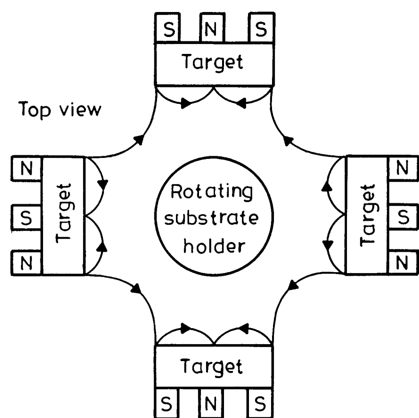

Fig. 1. Schematic diagram of four targets configuration used in the UDP450 sputtering apparatus.

2.2. Characterization of TiAlN films

The GD-OES composition analyzer (QDP GDS-750, LECO Co.) was used to analyze the chemical composition of deposited films. The operating voltage was 700 V, the current 20 mA. Scanning electron microscopy (SEM) was used for microstructural analysis. The phases and textures of deposited films were determined by X-ray diffraction (XRD) using Cu Kα radiation. The surface roughness of deposited film was measured with a Surfcorder 2300 analyzer. For each film, the average roughness value was taken from five test readings.

2.3. Mechanical properties

The surface hardness was measured with a Vickers microhardness tester (Akashi MVK-E) with an applied load of 50–1000 g for 15 s. For each specimen, the average hardness value was taken from at least nine test readings. To prevent the effects of substrate and film thickness on the film hardness, the equation derived by Thomas [14] was used to calculate the film's intrinsic hardness based on these micro-Vickers test readings. The interfacial adhesion was determined from the experiment of indentation testing, which was carried out using

a Rockwell (Mitutoyo AR-10) hardness tester, equipped with a Brale diamond indentor at applied loads of 60, 100 and 150 kgf. The dry sliding wear tests were performed using an ASTM G99-90 standard ball-on-disk type test machine. The SUJ-2 Cr-steel ball, with hardness $Hv=720$, was used as the against-wear material. The tests were conducted at a constant load of 30 N and a sliding speed of 31.4 cm/s. The average friction coefficient was monitored during the sliding wear process.

3. Results and discussion

3.1. Chemical composition

The chemical compositions of TiAlN films for specimen No. 2 were analyzed using GD-OES and the results are presented in Fig. 2. To increase the interfacial adhesion of TiAlN films by relaxing the lattice mismatch, both Ti and the following TiN interlayers were precoated on SKH51 substrate. In addition, the pre-coated TiN interlayer was expected to promote the growth of TiAlN films with the TiN (NaCl) structure, instead of with the AlN (ZnS) structure. The TiN (NaCl) structure exhibits a higher hardness than the AlN (ZnS) structure. As can be seen in Fig. 2, the compositions from the substrate to the outer surface are SKH51 substrate, TiN layer, Al ramping and TiAlN layer. The Ti/Al ratios of TiAlN films can be predicted from the sputtering parameters, involving the applied target currents, yielding of targets impinged by Ar ions and target configurations. The sputtered Ti/Al atoms are believed to be proportional to the applied target currents. The yielding of Ti atoms impinged by Ar ions was reported to be twice that of Al atoms [15]. Fig. 3 presents a comparison of the predicted and measured Ti fractions for various TiAlN films. The measured Ti fractions are for the most part close to those predicted. Carefully examining Fig. 3, under the same applied target currents, the Ti/Al ratio of TiAlN film increases with an increasing substrate bias, for example, No. 5 (120 V) > No. 6 (40 V) and No. 1 (60 V); No. 8 (90 V) > No. 7 (60 V). This phenomenon can be explained as follows: the backscattering of target atoms adhering to the substrate will increase with an increasing substrate bias. In addition, the backscattering of Al atoms is expected to be higher than that of Ti atoms, because Al atoms are lighter than Ti atoms. Hence, the Ti/Al ratio of TiAlN film can increase with an increasing substrate bias.

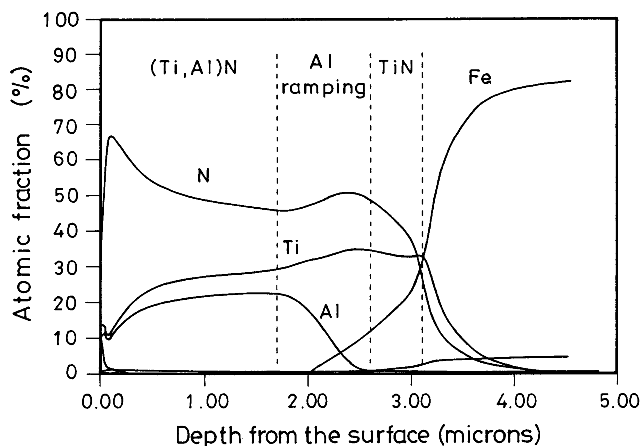

Fig. 2. The GD-OES analyzed composition diagram of TiAlN film for specimen No. 2.

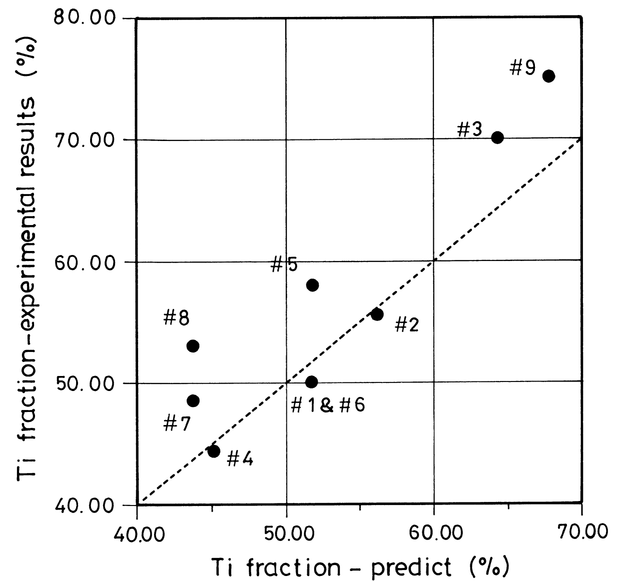

Fig. 3. The predicted and measured Ti fractions for various TiAlN films of specimens listed in Table 2.

3.2. Microstructure

Figs. 4 and 5 show the SEM photographs of the surface morphology for the TiAlN films with different composition and substrate bias, respectively. In Figs. 4 and 5, some porosities are observed on the film surface. The formation of these surface porosities can be explained as follows. During the sputtering process, the deposition of sputtered atoms initially induced the formation of island-type particles, which gradually diffuse and link together to form densely deposited films. During the final sputtering process, the incomplete linkage of island-type particles will appear in the surface porosity. As can be seen in Figs. 4 and 5, the chemical composition and substrate bias have no obvious effect on the quantity and size of surface porosity. Fig. 6 shows the surface roughness of deposited TiAlN film for the specimens listed in Table 2. In Fig. 6, the surface roughness of deposited TiAlN film is found to decrease with an increasing Ti fraction.

Typical SEM photographs illustrating the fractured cross-section of TiAlN films deposited at 60 V substrate

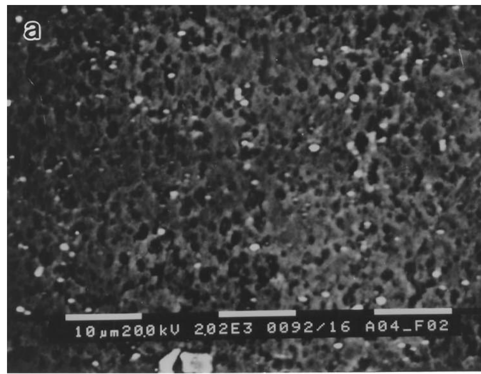

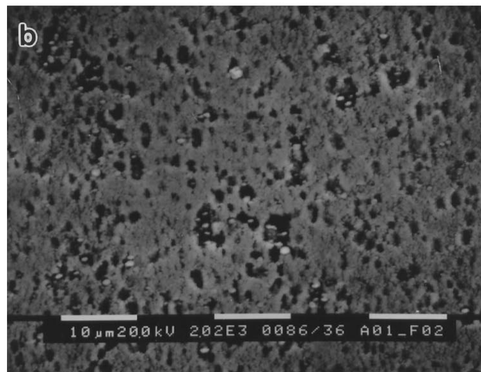

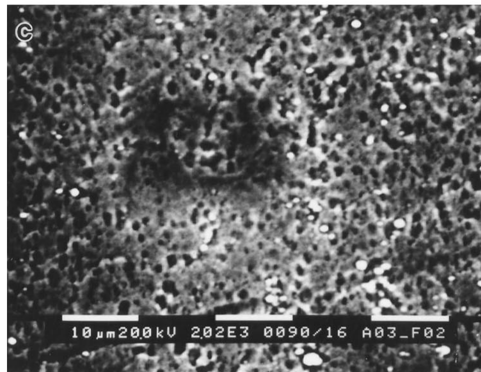

Fig. 4. SEM photographs of the surface morphology for the TiAlN films with Ti fractions of (a) 44.4 at%, (b) 50 at%, (c) 70 at%.

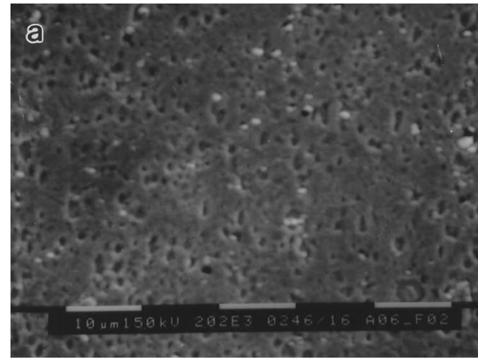

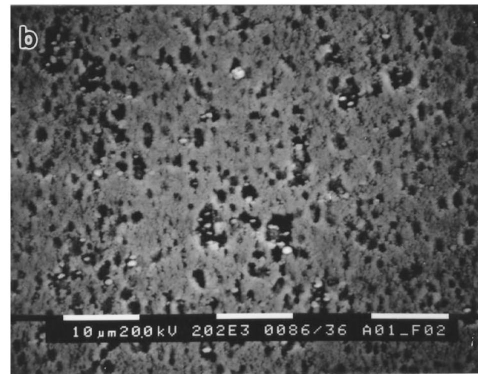

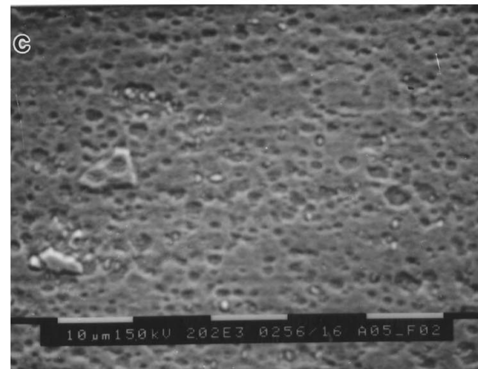

Fig. 5. SEM photographs of the surface morphology for the TiAlN films with substrate bias of (a) 40 V, (b) 60 V, (c) 120 V.

bias and with various Ti fractions are shown in Fig. 7. As can be seen in Fig. 7, the Ti/Al ratio has no obvious effect on the growth of TiAlN films. These TiAlN films exhibit a plainer surface with excellent substrate bonding. The TiAlN films deposited at 40 V and 120 V substrate bias are found to exhibit similar cross-sectional SEM photographs as those shown in Fig. 7, indicating that the substrate bias has no obvious effect on the growth of TiAlN films.

XRD patterns of TiAlN films with various Ti fractions, and with a comparative TiN film [16], are shown in Fig. 8. In Fig. 8, the TiAlN films mainly exhibit a δ-TiN structure, namely a NaCl cubic structure. Compared with the TiN film, the peak intensity of TiN(111) is lower than that of TiN(200) for most TiAlN films, except for the film with a 75% Ti fraction. Meanwhile, the peak intensity of TiN(200) is found to increase with a decreasing Ti fraction. These features indicate that the texture of δ-TiN structure will vary if the Ti atoms are partially replaced by Al atoms during the deposition of TiAlN films. For the TiN structure, (111) is the most close-packed plane and has the lowest surface energy. However, the (200) plane is not close-packed and has higher surface energy than the (111)

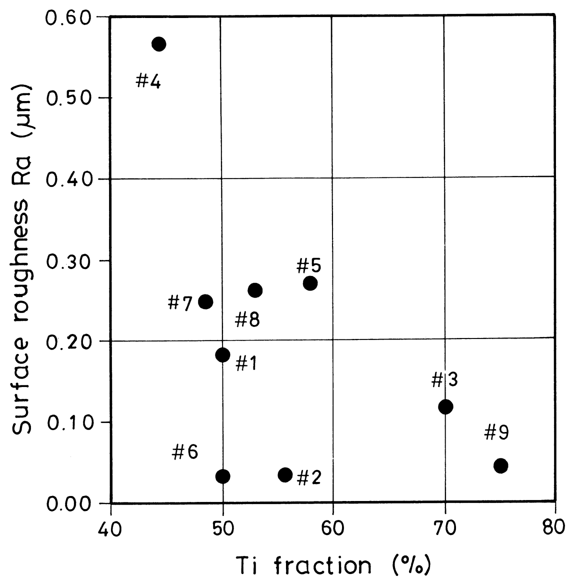

Fig. 6. The surface roughness of various deposited TiAlN films of specimens listed in Table 2.

plane. When Ti atoms are partially replaced by Al atoms, the induced strain energy on the (111) plane is higher than that on the (200) plane. Therefore, with a higher Al fraction, the total energy (surface energy and strain energy) of the (200) plane is lower than that of the (111) plane, resulting in the preferred texture of the (111) plane change to the (200) plane.

3.3. Mechanical properties

Fig. 9 shows the intrinsic hardness of various TiAlN films coated on SKH51 substrate. Ikeda and Satoh [17] reported that the hardness of TiAlN films increases with increasing Al fraction, and then decreases if the Al fraction was higher than 75%. However, as shown in Fig. 9, the intrinsic hardness of TiAlN films is randomly distributed. This feature may be ascribed to the composition heterogeneity, film thickness and δ-TiN texture variations of the TiAlN films deposited in this study. But the exact reason is not yet clear.

There are many methods to evaluate the adhesion of deposited film and substrate, involving the pull-off, shearing stress, indentation and scratch tests. In the present study, the indentation test was used to measure the adhesion of TiAlN film and SKH51 substrate. For the indentation test, the curve slope of lateral crack circle diameter vs. applied load can be used to decide the film's adhesion. A lower curve slope indicates a better adhesion [18].

Fig. 10 shows the experimental results of lateral crack diameter vs. applied load for TiAlN films with various Ti fractions of specimens listed in Table 2. The curved slopes at 100 and 150 kgf loads are used to judge their adhesion. As can be seen in Fig. 10, lower curve slopes

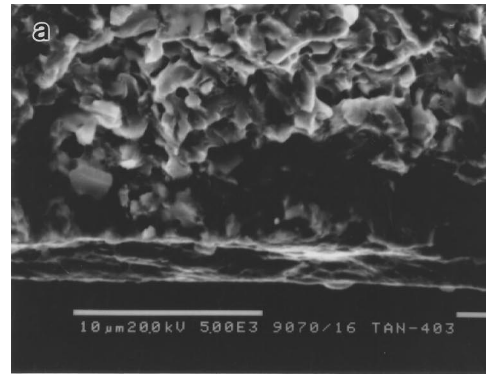

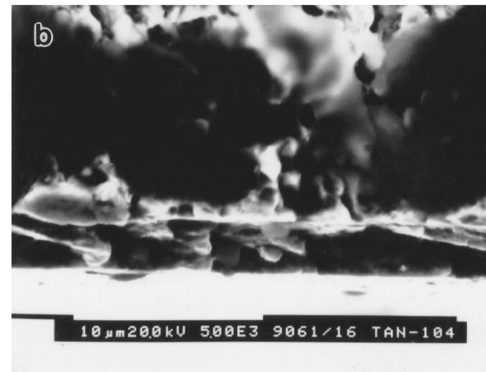

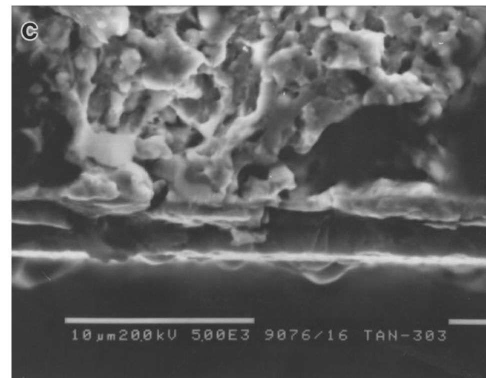

Fig. 7. SEM photographs illustrating the fractured cross-section of TiAlN films deposited at a substrate bias of 60 V and with Ti fractions of (a) 44.4 at%, (b) 50 at%, (c) 70 at%.

appear for the TiAlN films with 50–70% Ti fractions, indicating that the TiAlN films in the present study with 50–70% Ti fractions can exhibit a better adhesion property. To compare the adhesion property of TiAlN and that of TiN films [16] under the same sputtering condition, the pictures of a cracked circle for both TiAlN and TiN films are presented in Fig. 11(a) and (b), respectively. As can be seen in Fig. 11(a) and (b), the TiAlN film exhibits a flaking fracture, but the TiN film exhibits a cracking fracture. In addition, the TiAlN film

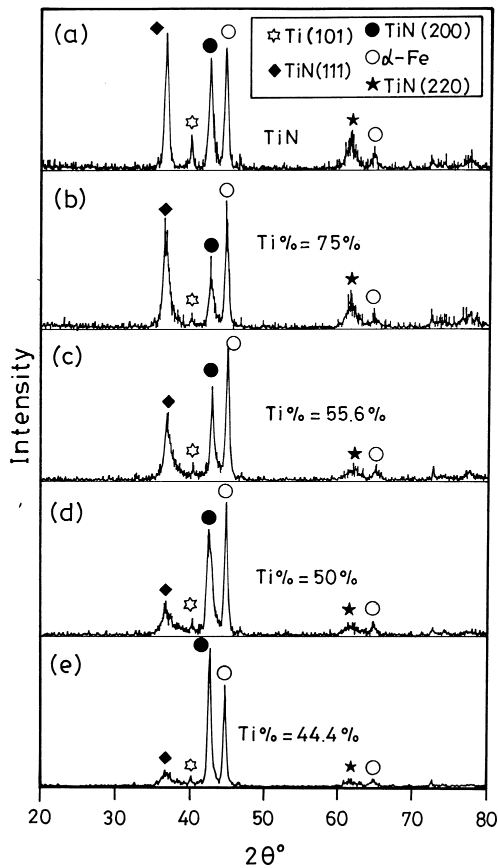

Fig. 8. (a) X-ray diffraction (XRD) patterns of deposited TiN film, and (b)–(e) TiAlN films with various Ti fractions.

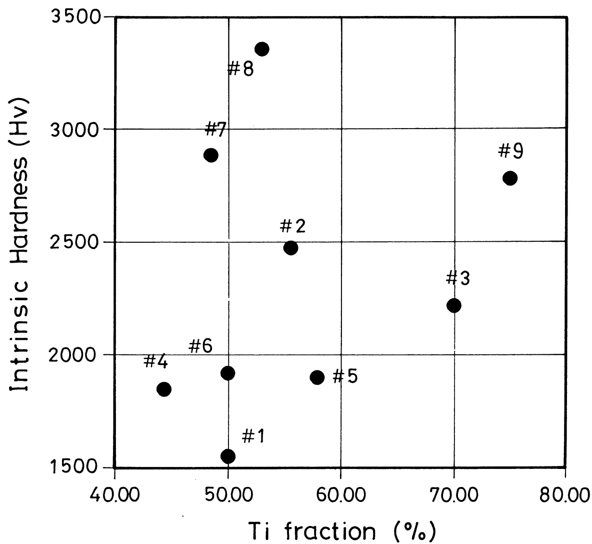

Fig. 9. The intrinsic hardness of various TiAlN films coated on SKH51 substrate. The intrinsic hardness is calculated according to Ref. [14].

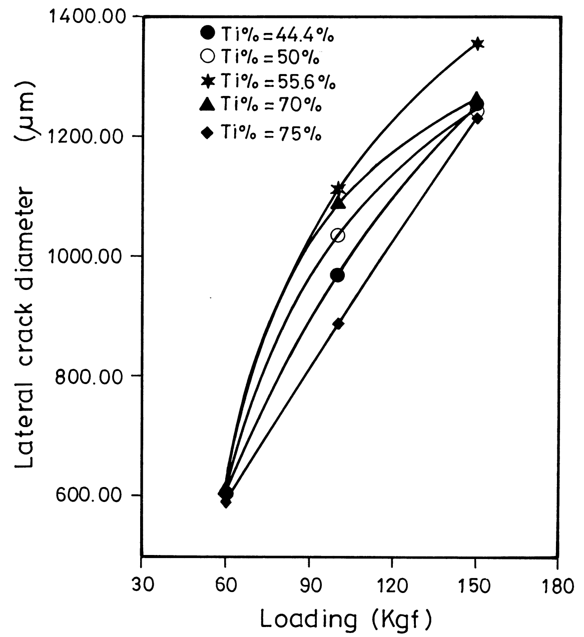

Fig. 10. The lateral crack diameter vs. applied load for TiAlN films with various Ti fractions.

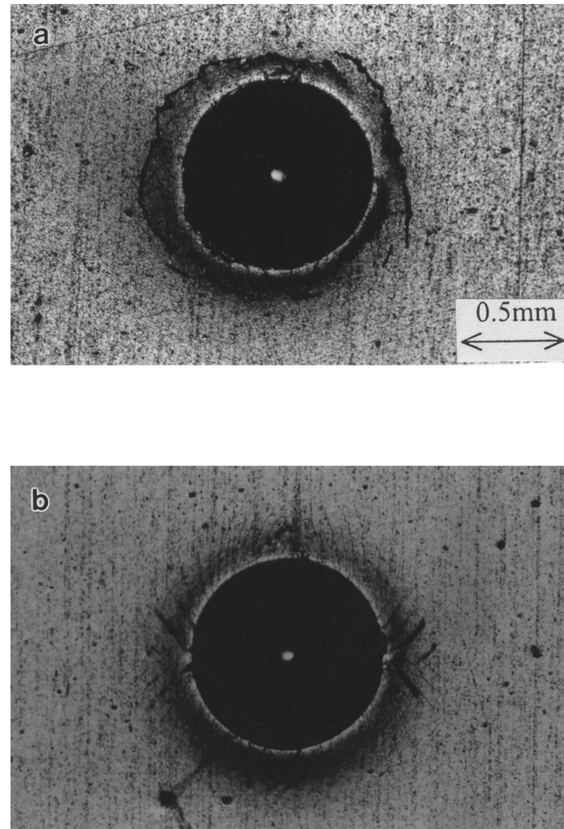

Fig. 11. The pictures of crack circle after a 150 kgf indentation test for (a) TiAlN film and (b) TiN film.

has a more severe fracture than can be seen in the TiN film. These features indicate that the TiAlN film exhibits an adhesion inferior to the TiN film [18], possibly due to the more internal stress occurring within the TiAlN films.

Fig. 12 shows the friction coefficients for specimens

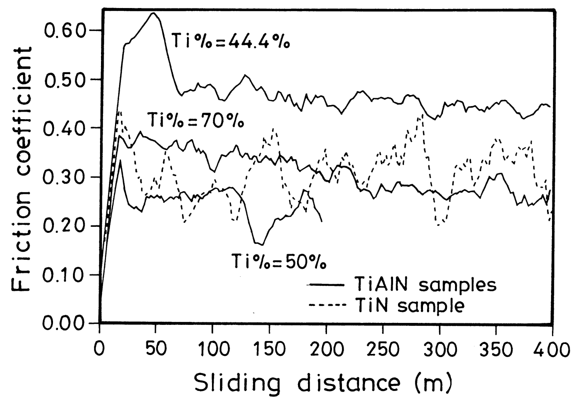

Fig. 12. The friction coefficients for specimens coated with various TiN and TiAlN films.

coated with TiN [16] and TiAlN films. The against-wear SKS-95 steel ($Hv=700$) is much softer than that of the TiN and TiAlN compounds; hence, both adhesive and abrasive wear occurs. The adhesive wear will cause fragments of SKS-95 steel to be pulled off and to adhere to the surface of the TiN and TiAlN films. This feature will degrade the cutting efficiency of a cutting tool coated with TiN or TiAlN films. In Fig. 12, the TiAlN film with a 50% Ti fraction exhibits the lowest friction coefficient, indicating that the TiAlN film with a 50% Ti fraction has the slightest adhesion of SKS-95 and hence will exhibit an excellent cutting performance.

4. Conclusions

The effects of substrate bias, target current and configuration of Ti/Al targets on the chemical composition, microstructure and mechanical properties of the unbalanced-magnetron sputtered TiAlN films have been investigated. The important conclusions are as follows.

1. The Ti/Al ratio of TiAlN films can be successfully predicted from the sputtering parameters, involving the applied target currents, yielding of targets impinged by Ar ions and target configurations.
2. When Ti atoms are partially replaced by Al atoms during the deposition, TiAlN films are identified as a δ-TiN structure and have the preferred texture of the (200) plane.
3. The worse adhesion of TiAlN films than that of TiN film under the same sputtering condition is suggested to come from the more internal stress occurring within the deposited TiAlN films.
4. The TiAlN film with 50% Ti fraction can exhibit an excellent cutting performance due to the slight adhesion of SKS-95 steel fragments during the cutting process.

Acknowledgements

The authors are pleased to acknowledge the financial support of this research by the National Science Council, Republic of China, under Grant NSC 82-0405-E002-402. The authors are also thankful to Dr. Y.S. Yang, Principle Investigator, Metals Industry R&D Centre, Kaoshiung, Taiwan, for his kind provision of the unbalanced-magnetron sputtering equipment.

References

[1] W.D. Munz, J. Vac. Sci. Technol. A 4 (6) (1986) 2717–2725.
[2] O. Knotek, W.D. Munz, T. Leyendecer, J. Vac. Sci. Technol. A 5 (4) (1987) 2173–2179.
[3] W. Konig, R. Fritsch, D. Kammermeier, Surf. Coat. Technol. 49 (1991) 316–324.
[4] T. Leyendecker, O. Lemmer, S. Esser, J. Ebberink, Surf. Coat. Technol. 48 (1991) 175–178.
[5] O. Knotek, T. Leyendecer, J. Solid State Chem. 70 (1987) 318–322.
[6] B.Y. Shew, J.L. Huang, D.F. Lii, Thin Solid Films 293 (1997) 212–219.
[7] B.Y. Shew, J.L. Huang, Surf. Coat. Technol. 73 (1995) 66–72.
[8] B. Window, N. Savvides, J. Vac. Sci. Technol. A 4 (2) (1986) 196.
[9] J.E. Sundgren, B.O. Johansson, S.E. Karlsson, Thin Solid Films 105 (1983) 353–393.
[10] A.J. Perry, M. Jagner, W.D. Sproul, P.J. Rudnik, Surf. Coat. Technol. 42 (1990) 49–68.
[11] D.S. Rickerby, P.J. Burnett, Thin Solid Films 157 (1988) 195–222.
[12] B.Y. Shew, J.L. Huang, Surf. Coat. Technol. 71 (1995) 30–36.
[13] D.P. Monaghan, D.G. Teer, K.C. Laing, I. Efeoglu, R.D. Arnell, Surf. Coat. Technol. 59 (1993) 21–25.
[14] A. Thomas, Surf. Eng. 3 (2) (1987) 117–122.
[15] R. Bunshah et al., Deposition Technology for Films and Coatings, Noyes Press, New Jersey, 1982, p. 109.
[16] P.L. Liu, Master Thesis, Institute of Materials Science and Engineering, National Taiwan University, Taipei, Taiwan, 1997.
[17] T. Ikeda, H. Satoh, Thin Solid Films 195 (1991) 99–110.
[18] P.C. Jindal, D.T. Quinto, G.J. Wolfe, Thin Solid Films 154 (1987) 362–375.